(%)Change in isotopic abundance ratio
$$= [(IAR_{Treated} - IAR_{Control})$$
$$/ IAR_{Control}] \times 100$$

(1)

Where $IAR_{Treated}$ is the isotopic abundance ratio of the treated sample and $IAR_{Control}$ is the isotopic abundance ratio of the control sample.

Gas Chromatography-Mass Spectrometry (GC-MS) Analysis: GC-MS of cholecalciferol was analyzed with the help of Perkin Elmer Gas chromatograph equipped with a PE-5MS (30M x 250 micros x 0.250 microns) capillary column and coupled to a single quadrupole mass detector was operated with electron impact (EI) ionization in positive mode. The oven temperature was maintained from 150°C (5 min hold) to 280°C (17 min hold) @ 10°C /min with a total run time of 35 min. The sample was prepared taking 50 mg of the cholecalciferol in 2.5 ml methanol as a diluent. The % change in the isotopic abundance ratios (P_{M+1}/P_M and P_{M+2}/P_M) for the Biofield Energy Treated cholecalciferol

compared to the control sample was calculated using the equation (1).

RESULTS & DISCUSSION

Liquid Chromatography-Mass Spectrometry (LC-MS)

A single major chromatographic peak of the control and treated cholecalciferol was observed at retention time (R_t) of 22.32 and 22.77 min, respectively **(Figure 1)**. This indicated that the polarity of both the samples was very close to each other.

The mass spectra of both the samples corresponding to the R_t ~22 min exhibited the presence of the molecular ion of cholecalciferol ($C_{27}H_{45}O^+$) adduct with hydrogen ion at *m/z* 385.25 (calcd for $C_{27}H_{45}O^+$, 385.35) along with the lower mass peak [M-OH]$^+$ at *m/z* 367.33 (calcd for $C_{27}H_{43}^+$, 367.3) **(Figures 2 and 3)**. The experimental data were well matched with the literature data [39].
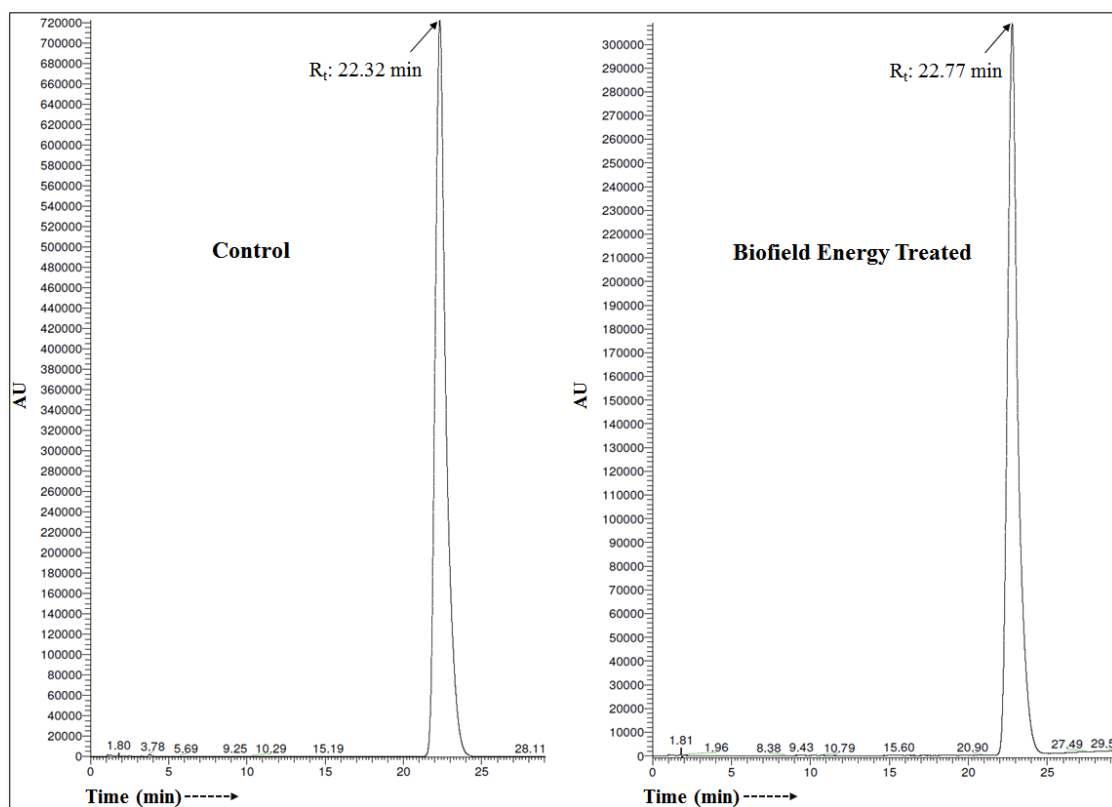
Figure 1. Liquid chromatograms of the control and Biofield Energy Treated cholecalciferol.

The cholecalciferol samples showed the mass of a molecular ion at *m/z* 385.25 with 100% relative abundance in the spectra. The theoretical calculation of isotopic peak P_{M+1} for the protonated cholecalciferol presented as below:

P (^{13}C) = [(27 x 1.1%) x 100% (the actual size of the M$^+$ peak)] / 100% = 29.7%

P (^{2}H) = [(45 x 0.015%) x 100%] / 100%= 0.675%

P (^{17}O) = [(1 x 0.04%) x 100%] / 100% = 0.04%

P_{M+1} *i. e.* ^{13}C, ^{2}H, and ^{17}O contributions from $C_{27}H_{45}O^+$ to *m/z* 386.25 = 30.42%
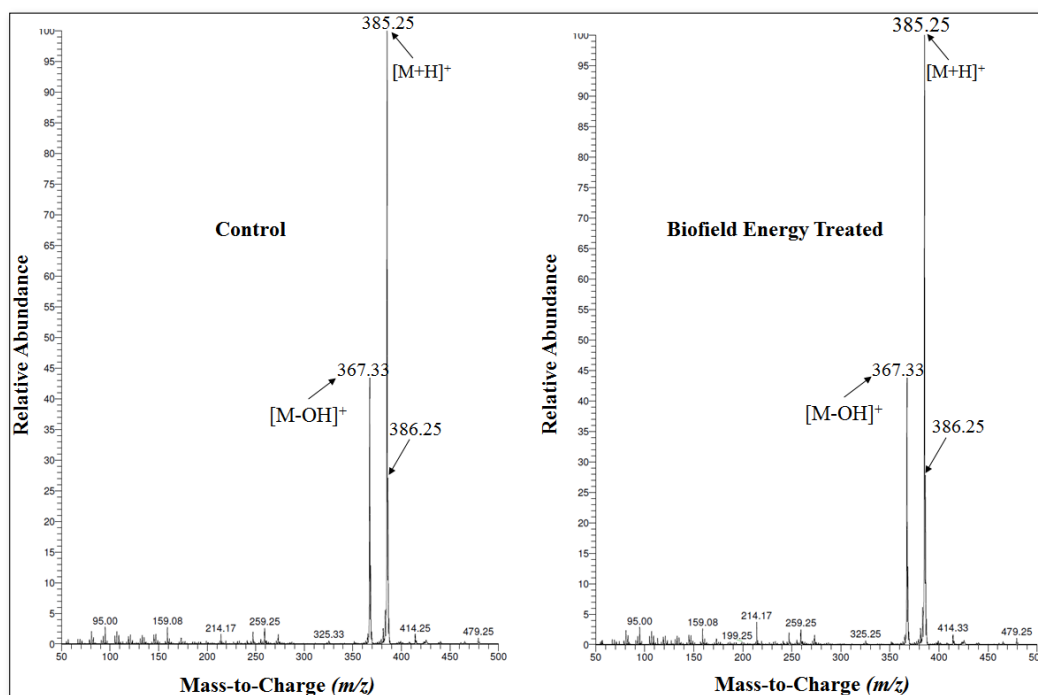
Figure 2. Mass spectra of the control and Biofield Energy Treated cholecalciferol.
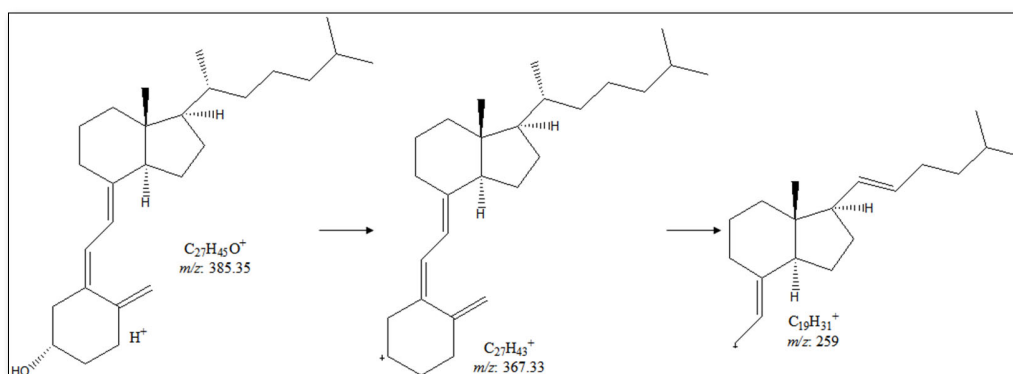

Figure 3. Proposed fragmentation pattern of cholecalciferol.

The calculated isotopic abundance of P_{M+1} value 30.42% was higher to the experimental value (27.76%) **(Table 1)**. From the above calculation, it has been found that ^{13}C has the major contribution to *m/z* 386.25.

The isotopic abundance ratio analysis P_M and P_{M+1} for cholecalciferol near *m/z* 385.25 and 386.25, respectively, which were obtained from the observed relative peak intensities of $[M^+]$ and $[(M+1)^+]$ peaks, respectively in the ESI-MS spectra **(Table 1)**. The isotopic abundance ratio of P_{M+1}/P_M ($^2H/^1H$ or $^{13}C/^{12}C$ or $^{17}O/^{16}O$) in treated cholecalciferol was increased by 2.93% compared to the control sample (Table 1). The result indicated that the ^{13}C, ^2H, and ^{17}O contributions from $C_{27}H_{45}O^+$ to *m/z* 386.25 in

the treated cholecalciferol was increased compared to the control sample.

Gas Chromatography-Mass Spectrometry (GC-MS) Analysis

The cholecalciferol samples showed two major independent peaks in the chromatograms **(Figures 4 and 5)**. The R_t of the control cholecalciferol was at 21.9 and 22.56 min, whereas 21.95 and 22.64 min is for the treated cholecalciferol, which indicated that the polarity of both the sample was very close **(Figures 4 and 5)**. The two prominent peaks in the chromatogram might be due to the *cis* and *trans* isomers of cholecalciferol in the sample [40,41].

Table 1. LC-MS based isotopic abundance analysis results in Biofield Energy Treated cholecalciferol compared to the control sample.

Parameter	Control sample	Biofield Energy Treated sample
P_M at *m/z* 385.25 (%)	100	100
P_{M+1} at *m/z* 386.25 (%)	26.97	27.76
P_{M+1}/P_M	0.27	0.28
% Change of isotopic abundance ratio (P_{M+1}/P_M) with respect to the control sample		2.93

P_M: the relative peak intensity of the parent molecular ion [M⁺]; P_{M+1}: the relative peak intensity of the isotopic molecular ion [(M+1)⁺], M: mass of the parent molecule

The molecular ion peak with respect to the R_t of 22 min exhibited the presence of cholecalciferol ($C_{27}H_{44}O^+$) at *m/z* 385 (calcd for $C_{27}H_{44}O^+$, 384.34). The low molecular mass fragmentation peak at *m/z* 367 $[C_{27}H_{43}]^+$ and 352 $[C_{26}H_{40}]^+$ were also observed in both the spectra **(Figures 4 and 5)**. The mass peak intensities of the Biofield Energy Treated cholecalciferol were altered compared to the control sample. The GC-MS spectra of both the cholecalciferol showed the mass of the molecular ion peak $[M]^+$ at *m/z* 385. The theoretical calculation of P_{M+1} and P_{M+2} for cholecalciferol was presented as below:

P (^{13}C) = [(27 x 1.1%) x 7.32% (the actual size of the M⁺ peak)] / 100% = 2.17%
P (^{2}H) = [(44 x 0.015%) x 7.32%] / 100%= 0.05%
P (^{17}O) = [(1 x 0.04%) x 7.32%] / 100% = 0.003%
P_{M+1} *i. e.*^{13}C, ^{2}H, and ^{17}O contributions from $C_{27}H_{45}O^+$ to *m/z* 386 = 2.22%

Similarly, the theoretical calculation of isotopic peak P_{M+2} for the protonated cholecalciferol was presented below:

P (^{18}O) = [(1 x 0.20%) x 7.32%] / 100% = 0.015%
P_{M+2} of ^{18}O contribution from $C_{27}H_{45}O^+$ to *m/z* 387 = 0.015%

The calculated isotopic abundance of P_{M+1} and P_{M+2} values were very close to the calculated value **(Table 2)**. From the above calculation, it has been found that ^{13}C and ^{18}O have major contribution to *m/z* 386 and 387 of cholecalciferol.

The GC-MS based isotopic abundance ratio analysis of the treated sample was calculated compared to the control sample. P_M, P_{M+1}, and P_{M+2} for cholecalciferol near *m/z* 385 $[M^+]$, 386 $[(M+1)^+]$, and 387 $[(M+2)^+]$, respectively of both the samples, which were obtained from the mass spectra. The isotopic abundance ratios of P_{M+1}/P_M and P_{M+2}/P_M in the treated sample was increased by 1.53% and 3.22%, respectively compared to the control sample **(Table 2)**. Therefore, the ^{13}C, ^{2}H, ^{17}O and ^{18}O contributions from $C_{27}H_{44}O^+$ to *m/z* 386 and 387 in the treated cholecalciferol were significantly increased compared with the control sample.
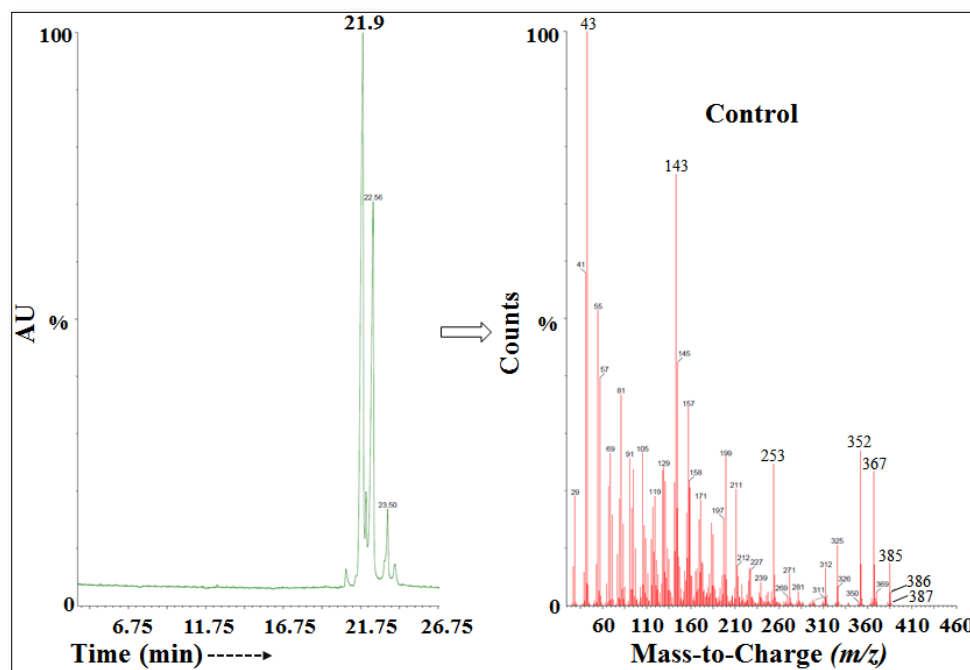
Figure 4. The GC-MS chromatogram and mass spectra of the control cholecalciferol.
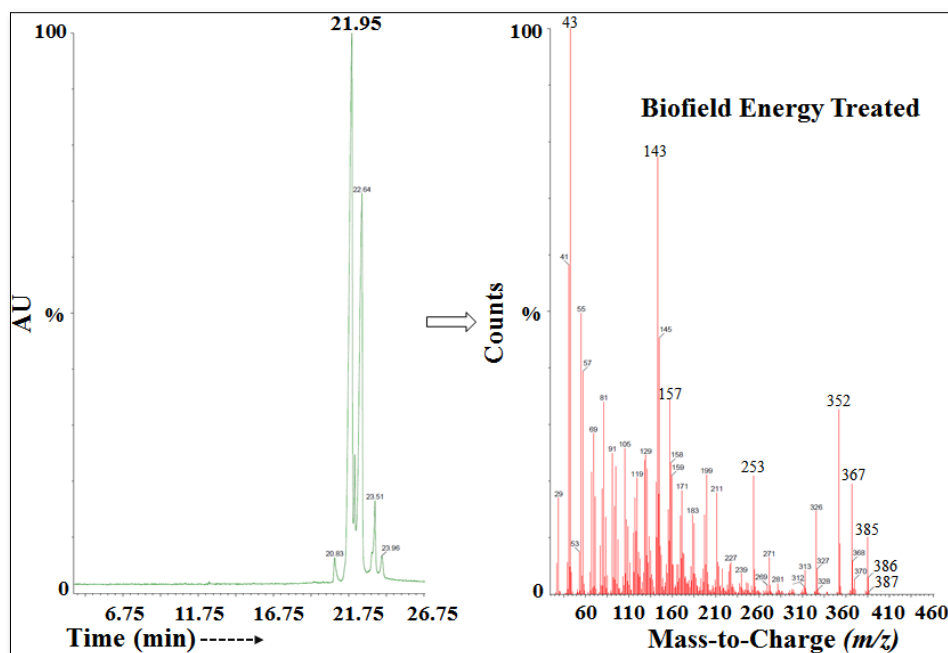
Figure 5. The GC-MS chromatogram and mass spectra of the Biofield Energy Treated cholecalciferol.

Table 2. GC-MS based isotopic abundance analysis results of Biofield Energy Treated cholecalciferol compared to the control samples.

Parameter	Control sample	Biofield Energy Treated sample
P_M at *m/z* 385 (%)	7.32	10.10
P_{M+1} at *m/z* 386 (%)	2.12	2.97
P_{M+1}/P_M	0.29	0.29
% Change of isotopic abundance ratio (P_{M+1}/P_M) compared to the control sample		1.53
P_{M+2} at *m/z* 387 (%)	0.33	0.47
P_{M+2}/P_M	0.05	0.05
% Change of isotopic abundance ratio (P_{M+2}/P_M) compared to the control sample		3.22

P_M: the relative peak intensity of the parent molecular ion [M⁺]; P_{M+1}: the relative peak intensity of the isotopic molecular ion [(M+1)⁺]; P_{M+2}: the relative peak intensity of the isotopic molecular ion [(M+2)⁺]; M: mass of the parent molecule

LC-MS and GC-MS study confirmed the structure of cholecalciferol. The isotopic abundance ratios of P_{M+1}/P_M ($^2H/^1H$ or $^{13}C/^{12}C$ or $^{17}O/^{16}O$) and P_{M+2}/P_M ($^{18}O/^{16}O$) in the treated cholecalciferol were increased compared to the control sample. The increased isotopic composition of the Consciousness Energy Healing Treated cholecalciferol might have interacted the neutron to proton ratio in the nucleus *via* the possible mediation of neutrino [15]. Neutrino is a subatomic particle abundantly found in the universe with no electrical charge and a very small mass. The neutrinos have the ability to interact with protons and neutrons in the nucleus, which might have a close relation between neutrino and the isotope formation [15, 34, 35]. The isotopic abundance ratios $^2H/^1H$ or $^{13}C/^{12}C$ or $^{17}O/^{16}O$ or $^{18}O/^{16}O$ would influence the atomic bond vibration of treated cholecalciferol [42]. The increased isotopic abundance ratio of the treated cholecalciferol may increase the intra-atomic bond strength, increase its stability, and shelf-life. The Trivedi Effect®-Consciousness Energy Healing Treated cholecalciferol would be more stable and suitable for the prevention and treatment of various diseases such as vitamin D deficiency, rickets, arthritis, osteoporosis, multiple sclerosis, cancer, diabetes mellitus, cardiovascular diseases, mental disorders, hypertension, infections, cognitive impairment in older adults, influenza, Parkinson's and Alzheimer's diseases, autoimmune disease, dementia, multiple sclerosis, glucose intolerance, etc.

CONCLUSIONS

The Trivedi Effect®-Consciousness Energy Healing Treatment has shown a significant impact on the isotopic abundance ratios of cholecalciferol. The LC-MS spectra of

both the samples at retention time (R_t) ~22 min exhibited the mass of the molecular ion peak at *m/z* 385.25 (calcd for $C_{27}H_{45}O^+$, 385.35). The LC-MS based isotopic abundance ratio of P_{M+1}/P_M in the Biofield Energy Treated cholecalciferol was increased by 2.93% compared with the control sample. Similarly, the GC-MS based isotopic abundance ratio of P_{M+1}/P_M and P_{M+2}/P_M in the Biofield Energy Treated cholecalciferol was increased by 1.53% and 3.22%, respectively compared with the control sample. Hence, ^{13}C, ^2H, ^{17}O, and ^{18}O contributions from $C_{27}H_{44}O^+$ to *m/z* 386 and 387 in the Biofield Energy Treated cholecalciferol were significantly increased compared with the control sample. The isotopic abundance ratios of P_{M+1}/P_M ($^2H/^1H$ or $^{13}C/^{12}C$ or $^{17}O/^{16}O$) and P_{M+2}/P_M ($^{18}O/^{16}O$) in the Biofield Energy Treated cholecalciferol were significantly increased compared to the control sample. The increased isotopic composition of the Trivedi Effect®-Consciousness Energy Healing Treated cholecalciferol might have altered the neutron to proton ratio in the nucleus *via* the possible mediation of neutrino. The increased isotopic abundance ratio of the Biofield Energy Treated cholecalciferol may increase the intra-atomic bond strength, stability, and shelf-life. The new form of cholecalciferol would be more efficacious pharmaceutical/nutraceutical formulations for the prevention and treatment of various diseases such as vitamin D deficiency, rickets, osteoporosis, arthritis, multiple sclerosis, cancer, mental disorders, diabetes mellitus, cardiovascular diseases, hypertension, infections, influenza, cognitive impairment in older adults, Parkinson's and Alzheimer's diseases, dementia, autoimmune disease, glucose intolerance, multiple sclerosis, etc.

ACKNOWLEDGEMENTS

REFERENCES

1. Kulie T, Groff A, Redmer J, Hounshell J, Schrager S (2009) Vitamin D: An Evidence-Based Review. J Am Board Fam Med 22: 698-706.

2. Nair R, Maseeh A (2012) Vitamin D: The "sunshine" vitamin. J Pharmacol Pharmacother 3: 118-26.

3. Coulston AM, Carol B, Mario F (2013) Nutrition in the prevention and treatment of disease. Academic Press. pp: 818.

4. Samuel S, Sitrin MD (2008) Vitamin D's role in cell proliferation and differentiation. Nutr Rev 66: S116-124.

5. Simana E, Simian R, Portnoy S, Jaffe, A, Dekel BZ (2015) Feasibility Study -Vitamin D loading

6. Ritu G, Gupta A (2014) Vitamin D Deficiency in India: Prevalence, Causalities and Interventions. Nutrients 6: 729-775.

7. Lawson DE, Wilson PW, Kodicek E (1969) Metabolism of vitamin D. A new cholecalciferol metabolite, involving loss of hydrogen at C-1, in chick intestinal nuclei. Biochem J 115: 269-277.

8. Ross CA, Taylor CL, Yaktine AL, Valle HBD (2010) Dietary reference intakes for calcium and Vitamin D. Washington (DC): National Academies Press (US); 2011. Accessed on: May 2, 2018. Available online at: https://pubmed.ncbi.nlm.nih.gov/21796828/

9. Koshy KT, Beyer WF (1984) Vitamin D3 (Cholecalciferol) in Analytical Profiles of Drug Substances, Florey K (Ed.), Vol 13, Academic Press, Inc., Orlando, USA, pp: 656-707.

10. Collins ED, Norman AW (2001) Vitamin D in Handbook of Vitamins, 3rd ed. Rucker RB, Suttie JW, McCormick DB, Machlin LJ, Marcel Dekker, Inc., New York, pp: 51-114.

11. Lehmann U, Hirche F, Stangl GI, Hinz K, Westphal S, et al. (2013) Bioavailability of vitamin D (2) and D (3) in healthy volunteers, a randomized placebo-controlled trial. J Clin Endocrinol Metab 98: 4339-4345.

12. Branton A, Jana S (2017) The use of novel and unique biofield energy healing treatment for the improvement of poorly bioavailable compound, berberine in male Sprague Dawley rats. Am J Clin Exp Med 5: 138-144.

13. Branton A, Jana S (2017) The influence of energy of consciousness healing treatment on low bioavailable resveratrol in male Sprague Dawley rats. Int J Clin Dev Anatomy 3: 9-15.

14. Branton A, Jana S (2017) Effect of the biofield energy healing treatment on the pharmacokinetics of 25-hydroxyvitamin D_3 [25(OH)D3] in rats after a single oral dose of vitamin D_3. Am J Pharmacol Phytother 2: 11-18.

15. Trivedi MK, Mohan TRR (2016) Biofield Energy Signals, Energy Transmission and Neutrinos. Am J Mod Phys 5: 172-176.

16. Rubik B, Muehsam D, Hammerschlag R, Jain S (2015) Biofield Science and Healing: History, Terminology, and Concepts. Global Adv Health Med 4: 8-14.

17. Warber SL, Cornelio D, Straughn, J, Kile G (2004) Biofield energy healing from the inside. J Altern Complement Med 10: 1107-1113.

determination by FTIR-ATR. Information & Control Systems 76: 107-111.

18. Movaffaghi Z, Farsi M (2009) Biofield therapies: biophysical basis and biological regulations? Complement Ther Clin Pr 15: 35-37.

19. Koithan M (2009) Introducing complementary and alternative therapies. J Nurse Pract 5: 18-20.

20. Barnes PM, Bloom B, Nahin RL (2008) Complementary and alternative medicine use among adults and children: United States, 2007. Natl Health Stat Report 12: 1-23.

21. Branton A, Trivedi MK, Nayak G, Trivedi D, Jana S (2018) Evaluation of the effect of biofield energy treatment on physicochemical and thermal properties of hydroxypropyl β-cyclodextrin. J Pharm Pharmacol 6: 5.

22. Nayak G, Trivedi MK, Branton A, Trivedi D, Jana S (2018) Evaluation of the effect of consciousness energy healing treatment on the physicochemical and thermal properties of selenium. J New Dev Chem 2: 13-23.

23. Nayak G, Trivedi MK, Branton A, Trivedi D, Jana S (2018) Evaluation of the physicochemical and thermal properties of chromium trioxide (CrO_3): Impact of consciousness energy healing treatment. Res Dev Mater Sci 8: 1-6.

24. Nayak G, Trivedi MK, Branton A, Trivedi D, Jana S (2018) Consciousness energy healing treatment: Impact on physicochemical and thermal properties of silver sulfadiazine. J Adv Pharm Sci Technol 2: 1-13.

25. Trivedi D, Trivedi MK, Branton A, Nayak G, Jana S (2019) Consciousness energy healing treatment: Impact on the physicochemical and thermal properties of ascorbic acid. Food Nutr Current Res 2: 164-173.

26. Trivedi MK, Branton A, Trivedi D, Nayak G, Sethi KK, et al. (2016) Isotopic abundance ratio analysis of biofield energy treated indole using gas chromatography-mass spectrometry. Sci J Chem 4: 41-48.

27. Trivedi MK, Branton A, Trivedi D, Shettigar H, Nayak G, et al. (2015) Assessment of antibiogram of multidrug-resistant isolates of *Enterobacter aerogenes* after biofield energy treatment. J Pharma Care Health Sys 2: 145.

28. Trivedi MK, Branton A, Trivedi D, Shettigar H, Nayak G, Gangwar M, et al. (2015) Antibiogram typing of biofield treated multidrug resistant strains of *Staphylococcus* species. Am J Life Sci 3: 369-374.

29. Trivedi MK, Patil S, Shettigar H, Mondal SC, Jana S (2015) The potential impact of biofield treatment on human brain tumor cells: A time-lapse video microscopy. J Integr Oncol 4: 141.

30. Trivedi MK, Patil S, Shettigar H, Gangwar M, Jana S (2015) *In vitro* evaluation of biofield treatment on cancer biomarkers involved in endometrial and prostate cancer cell lines. J Cancer Sci Ther 7: 253-257.

31. Trivedi MK, Branton A, Trivedi D, Nayak G, Mondal SC, et al. (2015) Evaluation of plant growth regulator, immunity and DNA fingerprinting of biofield energy treated mustard seeds (*Brassica juncea*). Agric Forest Fisheries 4: 269-274.

32. Trivedi MK, Branton A, Trivedi D, Nayak G, Bairwa K, Jana S (2015) Physical, thermal, and spectroscopic characterization of biofield energy treated murashige and skoog plant cell culture media. Cell Biol 3: 50-57.

33. Schellekens RC, Stellaard F, Woerdenbag HJ, Frijlink HW, Kosterink JG (2011) Applications of stable isotopes in clinical pharmacology. Br J Clin Pharmacol 72: 879-897.

34. Muccio Z, Jackson GP (2009) Isotope ratio mass spectrometry. Analyst 134: 213-222.

35. Weisel CP, Park S, Pyo H, Mohan K, Witz G (2003) Use of stable isotopically labeled benzene to evaluate environmental exposures. J Expo Anal Environ Epidemiol 13: 393-402.

36. Rosman KJR, Taylor PDP (1998) Isotopic compositions of the elements 1997 (Technical Report). Pure Appl Chem 70: 217-235.

37. Smith RM (2004) Understanding Mass Spectra: A Basic Approach, 2nd ed. John Wiley & Sons, Inc.

38. Jürgen H (2004) Gross Mass Spectrometry: A Textbook. 2nd ed. Springer: Berlin.

39. Predicted MS/MS Spectrum - 10V, Positive (Annotated) (DB00169). Available online at: https://www.drugbank.ca/spectra/ms_ms/61218

40. Holick MF, Garabedian M, DeLuca HF (1972) 5,6-Trans isomers of cholecalciferol and 25-hydroxycholecalciferol. Substitutes for 1,25-dihydroxycholecalciferol in anephric animal. Biochemistry 11: 2715-2719.

41. Okamura WH, Midland MM, Hammond MW, Abd Rahman N, Dormanen MC, et al. (1995) Chemistry and conformation of vitamin D molecules. J Steroid Biochem Mol Biol 53: 603-613.

42. Santesteban LG, Miranda C, Barbarin I, Royo JB (2014) Application of the measurement of the natural abundance of stable isotopes in viticulture: A review. Aust J Grape Wine Res 21: 157-167.